Environ. Sci. Technol. **2009,** *43,* 8684–8689

Bioelectrocatalysis of *Acetobacter aceti* and *Gluconobacter roseus* for Current Generation

R. KARTHIKEYAN, K. SATHISH KUMAR, M. MURUGESAN, SHEELA BERCHMANS,* AND V. YEGNARAMAN

Electrodics and Electro Catalysis Division, CSIR-CECRI, Central Electrochemical Research Institute, Karaikudi-630 006, India

Received July 7, 2009. Revised manuscript received September 16, 2009. Accepted October 6, 2009.

Acetobacter aceti and *Gluconobacter roseus*, which are known to be responsible for the spoilage of wine, are used for current generation in batch-type microbial biofuel cells and it has been shown for the first time that these two microorganisms do not require mediators for the transfer of electrons to the anode. Three biofuel cells were constructed with two cells containing the pure cultures of each of the microorganisms as the biocatalyst (A-MFC, G-MFC) and the third cell was constructed with the mixed culture of these two microorganisms as the biocatalyst (AG-MFC). The performance of the biofuel cells was evaluated in terms of open circuit voltage (OCV), fuel consumption rate, internal resistance, power output, and coulombic efficiency. The mixed culture cell (AG-MFC) exhibits a better overall performance compared to the other cells.

Introduction

Acetobacter aceti and *Gluconobacter roseus* belong to gram-negative prokaryotic species. Gram-negative prokaryotic cells have respiratory redox proteins located in the cell membrane and accessible from the periplasm. The outer membrane contains porins, which makes them permeable for a wide variety of low molecular weight charged mediators. A characteristic representative of prokaryotes frequently used for bioelectrochemical applications is the genera *Gluconobacter*. The periplasmic membrane bound pyrroloquinoline quinone (PQQ) containing enzymes of these genera provide fast and highly efficient oxidation of a wide variety of substrates. Alcohol dehydrogenase (ADH) of acetic acid bacteria, consisting of the genera *Acetobacter* and *Gluconobacter*, catalyzes the first step of acetic acid production, i.e., the oxidation of ethanol to acetaldehyde. ADH is a quinohemeprotein-cytochrome *c* complex bound to the periplasmic side of the cytoplasmic membrane and functions as the primary dehydrogenase in the ethanol oxidase respiratory chain, where ADH oxidizes ethanol by transferring electrons to ubiquinone embedded in the membrane phospholipids. So far, the mediated bioelectrocatalysis of these two microorganisms has been reported wherein quinone and a flexible osmium redox polyelectrolyte have been used as mediators (*1*−*4*). However the presence of the quinoheme protein-cytochrome C complex bound to the periplasmic side of the cytoplasmic membrane suggests that these microorganisms are likely to undergo direct electron transfer at the electrode surface. A proof of concept for this hypothesis has been provided in this paper by demonstrating the electrochemical activity of these two microorganisms through cyclic voltammograms recorded with glassy carbon electrode containing the biofilms of these microorganisms. Further, *Acetobacter aceti* is capable of oxidizing acetic acid to carbon dioxide. Hence the combination of these two species can be utilized for complete biodegradation of a fuel/carbon source. The presence of the membrane bound built-in mediators and the ability of *Acetobacter sp.* to break acetic acid to CO_2 are the key points for considering these two microorganisms for current generation. The efficiency of current generation using these microorganisms were evaluated separately and as a mixture in a two-compartment cell separated by a nafion membrane.

Experimental Section

MFC Constructions. Two-compartment microbial fuel cells (MFCs) were constructed by using Perspex plates where the proton exchange membrane (Nafion 115) was placed as a separator. The volume of each compartment was 125 mL. The pure cultures of *Acetobaceter aceti* (NCIM No. 2116) and *Gluconobacter roseus* (NCIM No. 2049) were procured from NCL, Pune, India. The subculturing of the microorganisms were carried out using the following media composition: tryptone (1 g), yeast extract (1 g), glucose (1 g),and $CaCO_3$ (1 g) in 100 mL of distilled water. Three MFCs have been constructed. In the cell A-MFC, *Acetobacter aceti* was used as the biocatalyst. In the cell designated G-MFC, *Gluconobacter roseus* was used as the biocatalyst. In the AG-MFC, a mixture of these two microorganisms was used as the biocatalyst (wet weight containing 0.4 g of *Acetobacter aceti* and 0.4 g of *Gluconobacter roseus*). In each cell, graphite felt (5 × 5 × 0.5 cm) was used as the anode and graphite sheet (5 × 5 × 0.5 cm) was used as the cathode. The anolyte consisted of centrifuged bacterial cells (wet weight of approximately 0.9 g) and glucose (5.6 mg/mL) in phosphate buffer medium (pH 7). Potassium ferricyanide (100 mM) in phosphate buffer (phosphate buffer: 8.6 g of KH_2PO_4, 1.2 g of NaOH in 1000 mL of distilled water) was used as catholyte. The anode compartments were kept strictly under deaerated conditions.

Formation of Biofilms on Glassy Carbon Electrode. The biofilm of a mixed culture (*Acetobacter aceti* and *Gluconobacter roseus*) was formed anodically on glassy carbon electrode (ϕ = 3 mm) under a constant current of 50 μA in phosphate buffer solution containing glucose (0.2 g/30 mL of buffer) and the mixed culture (wet weight of 0.1 g *Acetobacter aceti* and 0.1 g *Gluconobacter roseus*). Normal calomel electrode and Pt foil were used as a reference electrode and counter electrode, respectively. The electrode was subjected to this current polarization for a period of 7 days. After 7 days, the GC electrode was gently rinsed with fresh phosphate buffer solution and scanned in the potential region from −1 to +1 V under 50 mV/s in the phosphate buffer using NCE and Pt as reference and counter electrode, respectively, to analyze for biofilm formation.

Operations and Maintenance of MFCs. The three MFCs were operated at room temperature (28 ± 2 °C) for a period of 60 days. The cells were maintained under active working conditions by replacing the catholyte every 10 days and by adjusting the pH to neutral conditions whenever it fell below neutral pH. The microorganism suspended in the anode compartment was centrifuged and the phosphate buffer was freshly added and inoculated with the centrifuged cells whenever the cell OCV fell below 0.3 V. Due to consumption

* Corresponding author phone: +91-4565-227550 -407 (extension); e-mail: sheelaberchmans@yahoo.com.

10.1021/es901993y CCC: $40.75

Published on Web 10/21/2009

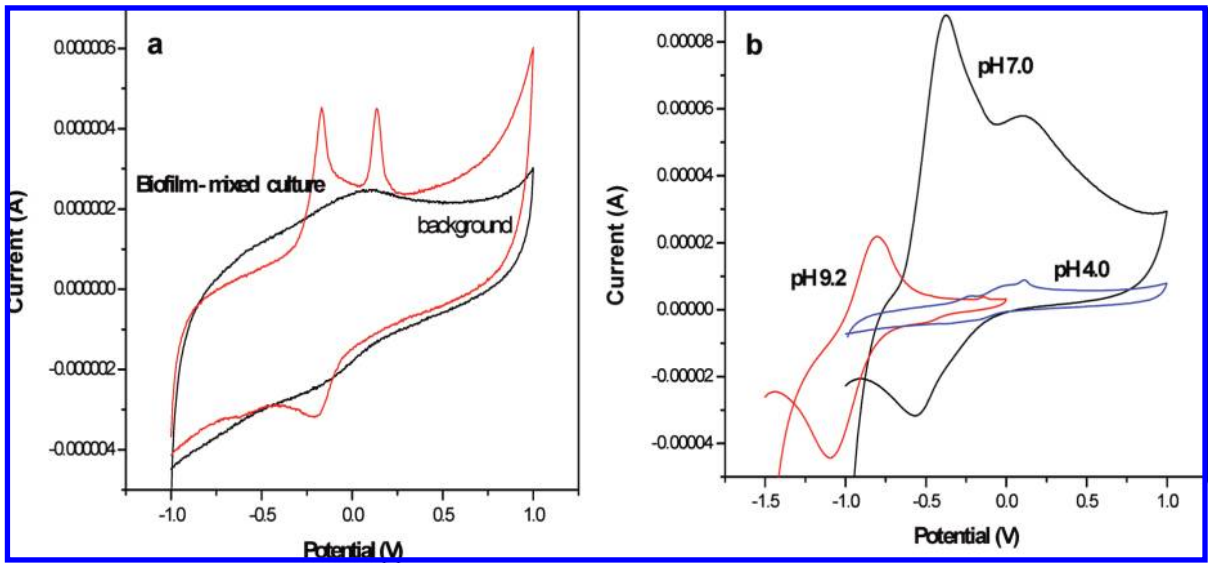

FIGURE 1. (a) Cyclic voltammograms representing the biofilm of the mixed culture and the background response. (b) pH dependence of the redox characteristics of the biofilm. Scan rate = 50 mV/s.

TABLE 1. Kinetics of Glucose Consumption under OCV Condition at the End of 6 Weeks

	A-MFC			G-MFC			AG-MFC		
day	OCV (V)	glucose (mg/mL)	loss of glucose per day (%)	OCV (V)	glucose (mg/mL)	loss of glucose per day (%)	OCV (V)	glucose (mg/mL)	Loss of glucose per day (%)
1	0.490	5.328	0	0.698	6	0	0.621	5.4	0
2	0.581	4.29	19.52	0.591	3.4	43.33	0.710	4.6	14.82
3	0.558	3.09	27.89	0.532	1.94	42.83	0.697	2.51	45.26
4	0.542	1.21	60.73	0.463	0.409 + 6[a]	78.91	0.680	1.31	47.64
5	0.504	0.592	51.07	0.403	3	50.07	0.707	0.7	46.57
6	0.523	0.444	25	0.585	1.3	56.67	0.705	0.5	28.57
8	0.564	0.148	33.34	0.509	1	11.54	0.695	0.2	30

[a] Since day 4 fuel content was low and it was increased to 6.4 mg/mL concentration.

TABLE 2. Kinetics of Glucose Consumption under Applied Load Condition at the End of 10 Weeks[a]

	A-MFC			G-MFC			AG-MFC		
day	potential (V)	glucose (mg/mL)	loss of glucose per day (%)	potential (V)	glucose (mg/mL)	loss of glucose per day (%)	potential (V)	glucose (mg/mL)	loss of glucose per day (%)
0	0.496	5.3	0	0.292	5.5	0	0.330	4.7	0
1	0.195	2.93	44.72	0.147	1.5	72.73	0.195	0.33	92.97
2	0.213	0.23096	92.12	0.123	0.15	90	0.213	0.2789	15.49
3	0.171	0.1 + 5.3[b]	56.702	0.132	0 + 6.1[b]	100	0.214	0.2 + 6.4[b]	28.29
4	0.182	1.7	68.51	0.112	1	83.60	0.199	2.1	68.18
5	0.221	0.384	77.41	0.091	0.128	87.2	0.179	0.2789	86.71
6	0.145	0.25056	34.75	0.069	0	100	0.161	0.26104	6.40
7	0.132	0.2168	13.47	0.069	0	0	0.159	0.256	1.93

[a] Applied resistance values: A-MFC 900 Ω, G-MFC 2000 Ω, AG-MFC 900 Ω. [b] Glucose was added on the third day to all the MFCs as the fuel level was very low.

of the fuel, at the end of the week, the voltage went down and we restored the OCV by adding fuel. The maximum OCV exhibited by the cell increased every week and the maximum OCV was reached after 6 weeks. During that period we could also see biofilm formation at the anode. After the formation of the biofilm, even if the cells were removed from the anolyte, they keep growing in the suspended state also. We could not avoid the formation of suspended microorganisms. Hence the biofilm and the suspended microorganisms are active. The fuel (glucose) levels were continuously monitored by spectrophotometry and the fuel was added when the consumption reached 90−95%.

Monitoring Glucose Concentration. Catalytic oxidation of fuel (glucose) by the microorganisms in the anolyte was analyzed by Cary 5000 UV-Vis-NIR spectrophotometer (Varian) at 490 nm. After the attainment of maximum open circuit voltage (OCV) regular analysis was carried out up to 8 days by phenol sulphuric acid method (*5*).

Polarization of MFCs by External Load. The polarization of MFCs was carried out by applying different external loads varying from 10000 Ω to 100 Ω. The resulting steady state voltage was recorded (*6*). The current output and power output were calculated from $I = V/R$ and $P = V^2/R$ and the power density was calculated in terms of anolyte volume (*7*).

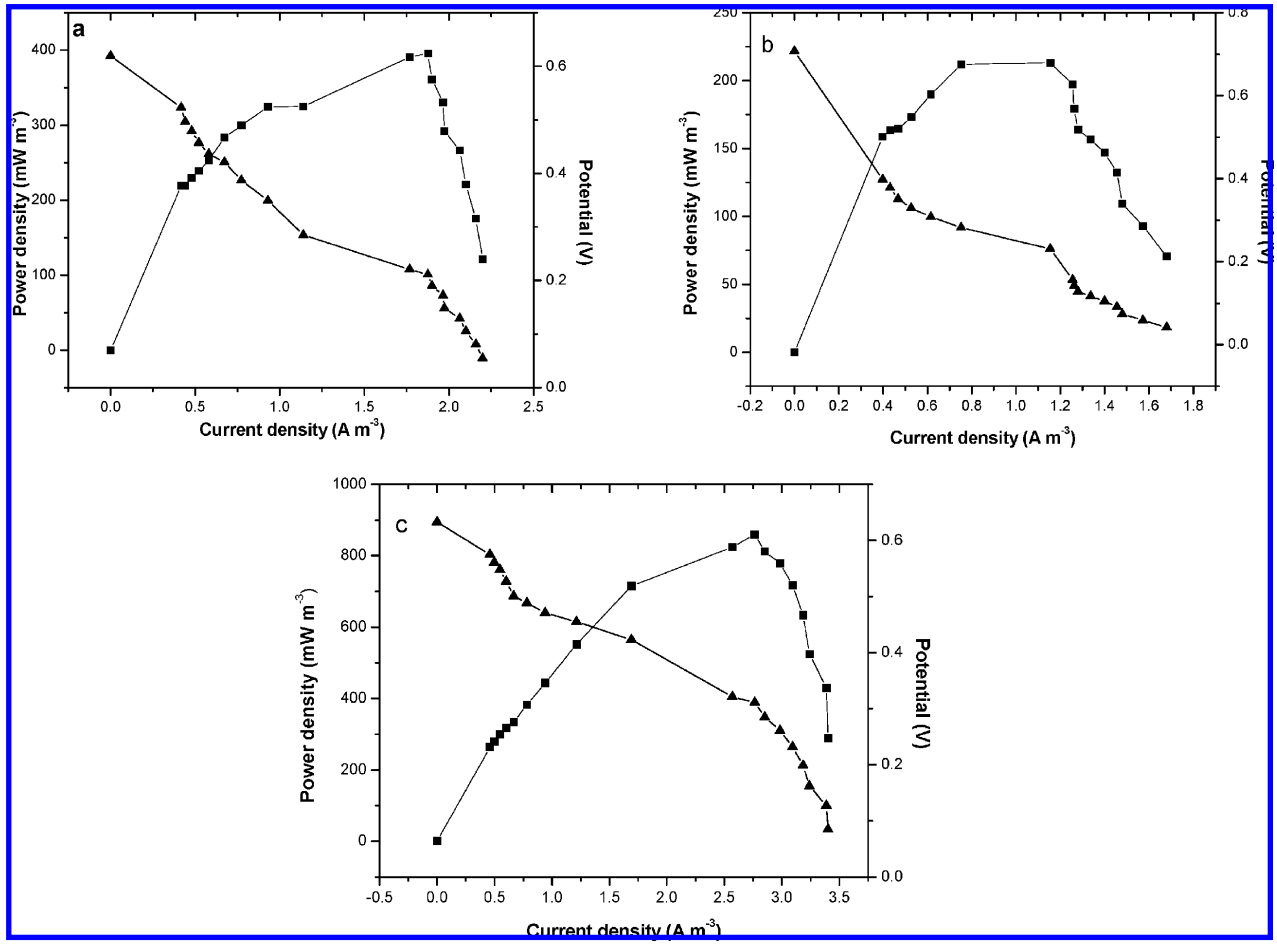

FIGURE 2. Polarization behavior of the MFCs: (a) A-MFC, (b) G-MFC, and (c) AG-MFC. ■ is power density; ▲ is potential.

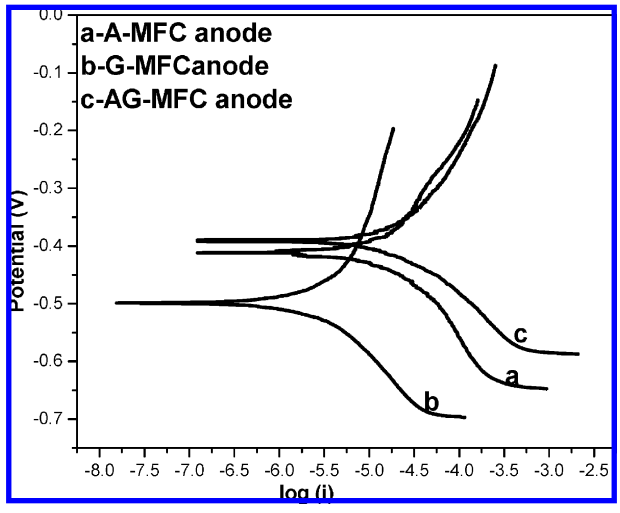

FIGURE 3. Potential sweep polarization (Tafel plot) curves of the three MFCs.

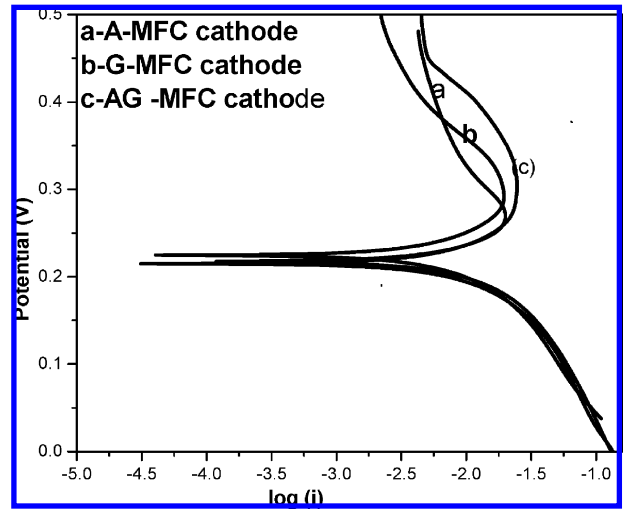

FIGURE 4. Potential sweep polarization (Tafel plot) curves of the three MFCs.

Internal resistance of the MFC was calculated from the slope of the polarization curve.

Electrochemical Characterizations. Electrochemical analyses of microbial fuel cells were carried out using PARSTAT 2263 electrochemical system. Potentiodynamic polarization (Tafel lines) of A-MFC, G-MFC, and AG-MFC anodes and cathodes were carried out from −250 mV to +250 mV at 0.5 mv/s from the open circuit potential (OCV) with respect to calomel electrode (NCE), where the anode was kept as the working electrode, NCE as the reference electrode, and cathode as the counter electrode. Same electrode configuration was used for galvanic sweep polarization (*8*) where the anodes were polarized from 10 to 1500 μA at 1 μA/s with the step time of 5 s. Both type of polarization resulted in similar performance of the anodes in the three cells.

Coulombic Efficiency. A, G, and AG-MFCs were discharged under the constant load of 25 Ω until the voltage reached 1% of OCV. Coulombic efficiency was calculated based on the following formula (*9, 10*):

$$\xi\% = Q_{obs}/Q_{theor} \times 100$$

TABLE 3. Tafel Constants Derived from Figure 3

anode	$E\ (I=0)$ (V)	exchange current density, I_0 (μA)	slope (anodic) b_a (mV/decade)	slope (cathodic) b_c(mV/decade)	polarization resistance R_p (Ω)
A-MFC	−0.394	77.62	225	206	602.38
G-MFC	−0.525	6.3	500	169	8716
AG-MFC	−0.381	131.8	200	150	282.75

TABLE 4. Tafel Constants Derived from Figure 4

cathode	$E\ (I=0)$ (V)	exchange current density, I_0 (mA)	slope (anodic) b_a (mV/decade)	slope (cathodic) b_c (mV/decade)	polarization resistance R_p (Ω)
A-MFC	0.281	8.97	76.2	181	2.59
G-MFC	0.25	7.49	104	181	3.83
AG-MFC	0.276	10	124	181	3.19

where Q_{obs} = current gained under constant load (C), Q_{theor} = quantity of current expected from the glucose consumption under constant load (C).

SEM Analysis of Microbial Growth. SEM analyses of the biofilms were carried out using the SEM unit Hitachi model-S-3000H. Biofilms of the three MFC anodes were scraped out with the help of a sterile glass rod and placed on a glass slide. The films were stained with 100 μL of phosphotungstic acid (0.5%) solution and SEM analysis was carried out.

Result and Discussion

Electrochemical Activity of the Biofilms of the Mixed Culture Formed on Glassy Carbon Electrode. The biofilm of the mixed culture formed on a glassy carbon electrode (as described in the experimental section) was characterized by cyclic voltammetry. Figure 1a represents the cyclic voltammogram of a bare glassy carbon electrode and that of the biofilm of the mixed culture formed on the glassy carbon electrode. The bare glassy carbon did not exhibit any redox features in phosphate buffer solution and the biofilm exhibited two anodic peaks at −0.163 and 0.137 V and one corresponding cathodic peak at −0.2 V. Figure 1b exhibits the pH dependence of the biofilm. At acidic pH the redox peaks shift in the positive direction. The anodic peak appearing at more positive potentials appear less predominant. At alkaline pH the redox peaks shift to the negative direction and the film exhibits a single redox peak. The redox peaks exhibit only quasi reversibility at all pH. The pH dependence of the redox potentials suggest the presence of pH dependent functional groups like quinones, flavins, etc. It is well-known that the periplasmic membrane bound pyrroloquinoline quinone (PQQ) containing enzymes of these genera of microorganisms *Gluconobacter roseus* and *Acetobacter aceti* provide fast and highly efficient oxidation of a wide variety of substrates. Hence it is concluded that the redox features of the biofilm can be assigned to the PQQ bound to the periplasmic membrane and it acts as the in built mediator for electron transfer and thus the electroactivity of the biofilm explains the direct electron transfer exhibited by these two microorganisms.

Kinetics of Fuel Consumption. The kinetics of fuel oxidation plays a major role for power delivery. Hence detailed analysis about the trends in the consumption of glucose was followed in the case of the three cells. The OCV reached the maximum value over a period of 6 weeks. The rate of glucose consumption was observed after 6 weeks and also after 10 weeks to evaluate the consistency in the pattern of consumption of glucose. At the end of 10 weeks, the kinetics

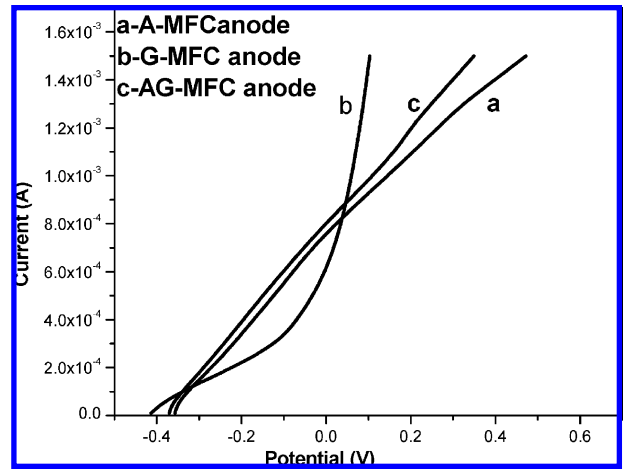

FIGURE 5. Galvanic sweep polarization curves of the three anodes.

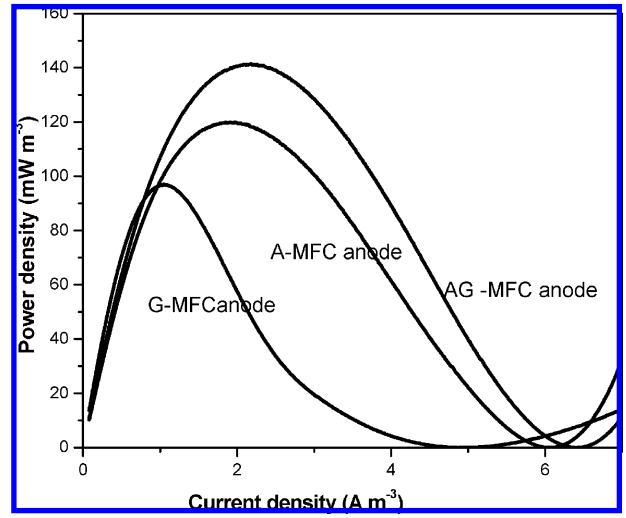

FIGURE 6. Power density vs current density curve plotted from the data derived from galvanic sweep polarization.

TABLE 5. Coulombic Efficiency with Respect to Fuel Oxidation or Consumption

system	discharged period (hrs)	Q_{obs} (C)	Q_{ther} (C)	ξ %
A-MFC	26.5	37.764	2187.96	1.7259
G-MFC	10.5	8.892	803.45	1.1067
AG-MFC	35.5	108.23	2326.79	4.65

of glucose consumption was investigated under open circuit conditions as well as under applied load conditions. The applied load was chosen from the polarization measurements. The load corresponds to the point where the maximum power density was obtained. Table 1 shows kinetics of glucose consumption with *Acetobacter aceti, Gluconobacter roseus*, and mixed culture observed after 6 weeks. The initial amount of glucose in the three fuel cells was found to be in the range of 5.3−6 mg/mL. In the case of A-MFC the consumption of glucose gradually increased up to day 4 and then decreased and also OCV increased to 0.564 V at the end of 8 days. The G-MFC fuel cell has higher consumption of glucose in the first 4 days (78.91%). Hence the concentration of glucose was again increased to 6.409 mg/mL by fresh addition of fuel. Then in the fifth and sixth day, the consumption of glucose was 50−56%. But in the eighth day the consumption of glucose dropped to 11.5%. The OCV value

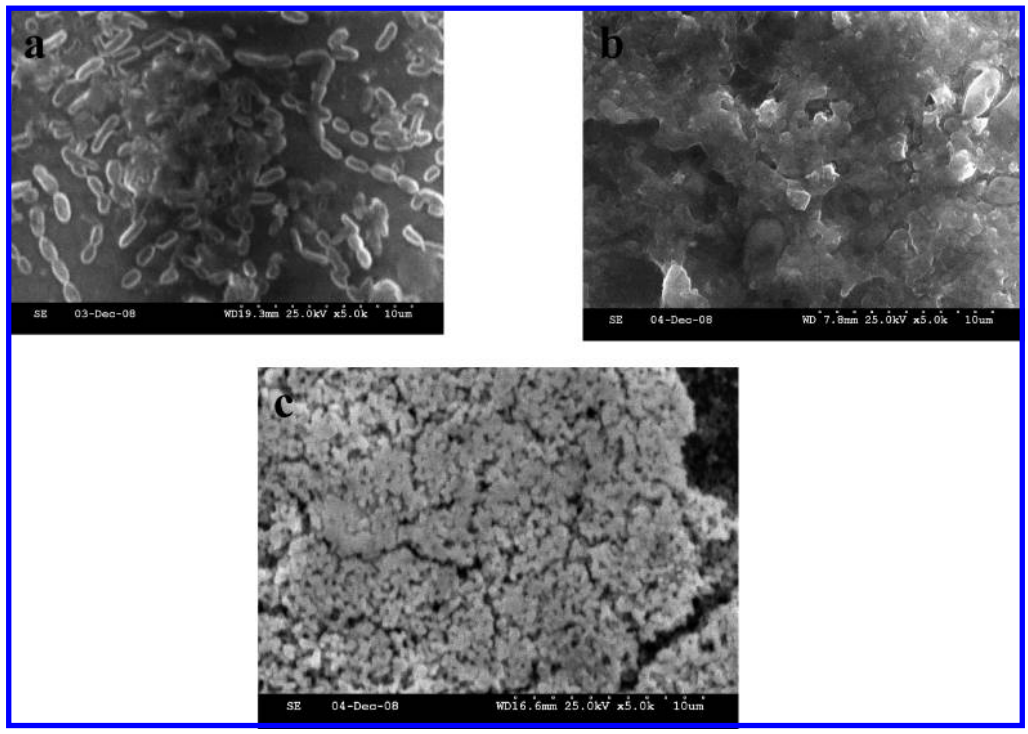

FIGURE 7. SEM images of biofilms obtained from the anodes: (a) A-MFC, (b) G-MFC, (c) AG-MFC.

has decreased from 0.698 to 0.509 V on the eighth day. But in the case of *Acetobacter aceti* fuel cell the OCV was steadily increasing with respect to the consumptions of glucose. In the case of mixed culture fuel cell the loss of glucose was in the range of 45−47% in five days and also the OCV increased from 0.621 to 0.707 V and in the subsequent days OCV decreased to 0.695 V. From the overall data, it is inferred that the A-MFC fuel cell exhibited 97.22% of glucose consumption. In the case of the *Gluconobacter* fuel cell the glucose consumption was 93.18% in the first 4 days and after glucose replenishment the consumption was 88.79% (days 5−8). In the case of the mixed culture fuel cell the glucose consumption was 96.3% in 8 days.

The kinetics of consumption of glucose after 10 weeks was nearly similar to that observed at 6 weeks (see Supporting Information Table S1). The pattern of consumption of glucose observed in the presence of applied load at the end of 10 weeks is given in Table 2. In presence of the load, it can be clearly seen that the glucose consumption is faster. Within 2 days the consumption of glucose has reached ≥90% in the case of A-MFC and G-MFC and in the case of AG-MFC, the consumption reached 90% within a day. Additional fuel was added on the third day to all the MFCs.

Polarization of the Fuel Cell by External Load. The fuel cells were polarized by external resistances varying from 10000 Ω to 100 Ω. After applying a particular external load, the resulting steady state voltage was recorded. The next resistance was applied after the attainment of the initial OCV (±20 mV). Figure 2a−c describe results of the polarization experiments. A-MFC fuel cell yields the maximum power density of 395.74 mW m^{-3} at 1.8755 A m^{-3}, G-MFC fuel cell yields only 213.14 mW m^{-3} at 1.155 A m^{-3}, and the mixed culture fuel cell yields the maximum of 859.74 mW m^{-3} at 2.7644 A m^{3-}. It has been discussed in the literature (*11*) that the power output of the MFC was mainly affected by Ohmic resistance whereas that of the chemical fuel cell was affected by mass transfer. The polarization curves are not linear, so the slopes of polarization curve were not strictly equal to that of internal resistance. The Ohmic resistance can be measured as the slope of the midpart of the polarization curves (*11*). In the case of the A-MFC, the potential region from 0.349 to 0.211 V has the slope value of 1168 Ω. The G-MFC shows a slope value of 1397 Ω in the potential region between 0.351 and 0.231 V. The mixed culture fuel cell (AG-MFC) shows 835 Ω in the potential region between 0.423 and 0.311 V. This indicates that mixed culture fuel cell has low R_Ω compared to other two fuel cells and it generates high power. Moreover *Gluconobacter* fuel cell (G-MFC) has low power density and high Ohmic resistance (R_Ω). It should be pointed out that if the fuel (glucose) was not completely oxidized by microorganism the H^+ concentration production in the anolyte becomes lower. When the amount of H^+ ion is low, the movement of H^+ ions toward membrane became limited and get dominated by other cations by 10^4 times (*12*−*14*).

Electrochemical Characterizations of Anodes. *Potentiodynamic Polarization.* Potentiodynamic polarization of MFC anodes will provide useful information about kinetics of the half cell reaction. Figures 3 and 4 show Tafel plots of the three anodes and cathodes. Tables 3 and 4 depict the results obtained from the Tafel plots. The parameters that can be derived from the Tafel plot are exchange current density (i_0), anodic Tafel slope (b_a), and polarization resisatnce (R_p). The polarization behaviors of the three anodes reveal that the E ($I = 0$) value of mixed culture anode is lower compared to that of the *Acetobacter aceti* and *Gluconobacter* anodes. I_0 of AG-MFC anode has a higher value of 131.8 μA (1.0544 A m^{-3}) whereas A-MFC anode exhibits a value of 77.62 μA (0.6209 A m^{-3}) and G-MFC anode exhibits a value of 6.3 μA (0.0504 A m^{-3}). In terms of anodic electron transfer coefficient (b_a), AG-MFC anode exhibits a lower value of 200 mV/decade than that of other anodes. The R_p value obtained for G-MFC anode is of high magnitude 8716 Ω, whereas A-MFC anode and AG-MFC anode exhibit a R_p of 602.38 Ω and 282.75 Ω, respectively. The anodic reaction will be facilitated when b_a and R_p are low and I_0 is high. Based on the results obtained, the AG -MFC anode exhibits facile electron transfer kinetics compared to the other anodes (*15*). Similarly the polarization behavior of the cathodes of the three MFC were analyzed. Analysis shows that cathodic reaction is an activation controlled process. The Tafel parameter (Table 4) indicates these three cathodes have similar performances in terms of E_0 (0.25−0.28 V), I_0 (7.5−10

mA), b_a (75−125 mV/dec), b_c (181 mV/dec), and R_p (2.5−3.2 Ω). Since these cathodes exhibit high exchange current density (I_0) and lower polarization resistance (R_p), it is confirmed that power delivery is not limited by these cathodes.

Galvanic Sweep Polarization. Figure 5 represents the galvanic polarization curves obtained from three anodes of fuel cells. The anodes were polarized by applying different current steps as explained in the experimental section and the corresponding potential changes at the anode with respect to a calomel electrode (1 N KCl) were recorded. Figure 6 was obtained using the data from Figure 5. From the results at steady state voltage, the corresponding values of power density are evaluated ($V \times I/v$ where V is the voltage of the anode, I is the applied current, and v is the volume of the anolyte). Figure 6 clearly reveals that the highest anodic power density of 140.49 mW m^{-3} at 2.148 A m^{-3} was obtained from AG-MFC anode. A-MFC anode shows 119.41 mW m^{-3} of anodic power density at 1.1935 A m^{-3}, which was higher than G-MFC anode exhibiting a power density of 96.29 mW m^{-3} at 1.0854 A m^{-3}.

Coulombic Efficiency with Respect to Fuel Loss. Coulombic efficiency is a main criterion for practical application of microorganisms for power generation. Table 5 shows the calculated Coulombic efficiency of three MFCs. The period of discharge (as evaluated by the time required for the voltage to reach 1% of its initial OCV) varied from 10.5 to 35.5 h for the three biofuel cells. The lowest Coulombic efficiency was noted for G-MFC since it produced the lowest charge generation (803.45 C) under the load conditions. A-MFC yielded a slightly higher Coulombic efficiency of 1.726%. Interestingly, the mixed culture fuel cell (AG-MFC) shows Coulombic efficiency of 4.65%. From Table 1 we noticed that the consumption of glucose was highest in *Gluconobacter* fuel cell but Coulombic efficiency was found to be low. This indicates that the *Gluconobacter* utilizes more fuel for fermentation and the rate at which electrons are transferred to the anode is comparatively low and hence it exhibits lower Coulombic efficiency. The Coulombic efficiency of A-MFC was slightly higher compared to G-MFC. In the case of AG-MFC, the Coulombic efficiency was still higher compared to the other two cases.

SEM Images of MFCs Biofilm on Anode. Figure 7a−c shows the SEM images of biofilms obtained from the three MFCs. The features of the microorganisms are clearly visible in the case of *Acetobacter aceti*, whereas in the other two cases prolific growth of microorganisms is observed and the individual features of the microorganisms are not clearly evident from the SEM pictures.

In conclusion, three batch type, two-compartment biofuel cells, A-MFC, G-MFC, and AG-MFC, were systematically evaluated for their performance in terms of OCV, fuel consumption, power output, internal resistance, and Coulombic efficiency. Higher OCV values were obtained in the case of AG-MFC and G-MFC cells. In the case of fuel consumption, G-MFC exhibited highest performance. However, in terms of Coulombic efficiency, the mixed culture cell AG-MFC showed a better performance. With respect to internal resistance, G-MFC cell exhibited a very high value. This is a probable reason for its low Coulombic efficiency though the fuel consumption efficiency was highest. The power output was very much higher in the case of the mixed culture AG-MFC cell. The low internal resistance combined with a reasonably good consumption rate of glucose and a higher OCV are responsible for the better performance of the mixed culture cell AG-MFC. Hence a mixed culture of the microorganisms *Gluconobacter roseus* and *Aceobacter aceti* has resulted in better performance of the biofuel cells constructed by us. Another interesting feature demonstrated in this work is the absence of mediators for current generation. Hence the combination of these two species can be used for the complete degradation of sugars and hence can be used in distilleries and breweries for current generation.

Acknowledgments

We thank the Ministry of New and Renewable Energy, New Delhi, India for funding this research work.

Supporting Information Available

Table S1 provides details of the kinetics of glucose consumption of the three biofuel cells under open circuit conditions at the end of 10 weeks; Figures S1 and S2 depict the electrochemical activity of the pure culture *Acetobacter aceti* and *Gluconobacter roseus*. This material is available free of charge via the Internet at http://pubs.acs.org.

Literature Cited

(1) Vostiar, I.; Ferapontova, E. E.; Gorton, L. Electrical "wiring" of viable *Gluconobacter oxydans* cells with a flexible osmium-redox polyelectrolyte. *Electrochem. Commun.* **2004**, *6*, 621–626.
(2) Ikeda, T.; Kato, K.; Tatsumi, H.; Kano, K. Mediated catalytic current for the oxidation of ethanol produced by *Acetobacter aceti* cells suspended in solution. *J. Electroanal. Chem.* **1997**, *440*, 265–269.
(3) Ikeda, T.; Kato, K.; Maeda, M.; Tatsumi, H.; Kano, K.; Matsushita, K. Electrocatalytic properties of *Acetobacter aceti* cells immobilized on electrodes for the quinone-mediated oxidation of ethanol. *J. Electroanal. Chem.* **1997**, *430*, 197–204.
(4) Takayama, K.; Kurosaki, T.; Ikeda, T. Mediated electrocatalysis at a biocatalyst electrode based on a bacterium *Gluconobacter industrius*. *J. Electroanal. Chem.* **1993**, *356*, 295–301.
(5) Sadasivan, S.; Manickam, A. *Biochemical Methods*, 2nd ed.; New Age International (P) Limited Publishers: New Delhi, 1996.
(6) Hoogers, G., Ed. *Fuel Cell Technology Handbook*; CRC Press: Boca Raton, FL, 2003.
(7) Bullen, R. A.; Arnot, T. C.; Lakeman, J. B.; Wash, F. C. Biofuel cells and their development. *Biosens. Bioelectron.* **2006**, *21*, 2015–2045.
(8) Zhao, F.; Harnisch, F.; Schrder, U.; Scholz, F.; Bogdanoff, P.; Herrmann, I. Challenges and constraints of using oxygen cathodes in microbial fuel cells. *Environ. Sci. Technol.* **2006**, *40* (17), 5193–5199.
(9) Heijne, A. T.; Hamelers, H. V. M.; Wilde, V.; Rozendal, R. A.; Buisman, C. J. N. A bipolar membrane combined with ferric iron reduction as an efficient cathode system in microbial fuel cells. *Environ. Sci. Technol.* **2006**, *40*, 5200–5205.
(10) You, S.; Zhao, O.; Zhang, J.; Jiang, J.; Zhao, S. A microbial fuel cell using permanganate as the cathodic electron acceptor. *J. Power Source* **2006**, *162*, 1409–1415.
(11) Logan, B. E.; Hamelers, B.; Rozendal, R.; Schroder, U.; Keller, J.; Freguia, S.; Aelterman, P.; Verstraete, W.; Rabaey, K. Microbial Fuel Cells: Methodology and Technology. *Environ. Sci. Technol.* **2006**, *40*, 5181–5192.
(12) Manohar, A. K.; Bretschger, O.; Nealson, K. H.; Mansfeld, F. The polarization behavior of the anode in a microbial fuel cell. *Electrochim. Acta* **2008**, *53*, 3508–3513.
(13) Samec, Z.; Trojanek, A.; Langmaier, J.; Samcova, E. Diffusion coefficients of alkali metal cations in Nafion from ion-exchange measurements - an advanced kinetic model. *J. Electrochem. Soc.* **1997**, *144*, 4236–4242.
(14) Stenina, I. A.; Sistat, P.; Rebrov, A. I.; Pourcelly, G.; Yaroslavtsev, A. B. Ion mobility in Nafion-117 membranes. *Desalination* **2004**, *170*, 49–57.
(15) Rozendal, R. A.; Hamelers, H. V. M.; Buisman, C. J. N. Effects of membrane cation transport on pH and microbial fuel cell performance. *Environ. Sci. Technol.* **2006**, *40*, 5206–5211.

ES901993Y